Pramāṇa, Vol. 23, No. 4, October 1984, pp. 495–500. © Printed in India.

Elastic scattering of 36 MeV alpha particles from ^{197}Au

S KAILAS, S K GUPTA, S BHATTACHARYA,**
S N CHINTALAPUDI* and Y P VIYOGI*

Nuclear Physics Division, Bhabha Atomic Research Centre, Bombay 400 085, India
*Variable Energy Cyclotron Centre, **Nuclear Physics Division,
Bhabha Atomic Research Centre, Calcutta 700 064, India

MS received 30 April 1984

Abstract. Angular distribution for the elastic scattering of 36 MeV alpha particles from gold target has been measured from $\theta \sim 10$–56°. The cross-section data have been analyzed in terms of the optical model. The real part of the optical model potential (V_R) has been deduced by two prescriptions: (i) combining the volume integral, the radius at which $V_R = 2{\cdot}4$ MeV and the slope at this radius $(1/V_R)(dV_R/dr)$ (ii) combining the volume integral, the root mean square radius and the equivalent sharp radius systematics. The imaginary potential depth has been searched to fit the data. The prediction using (i) for the real potential fits the data the best.

Keywords. Elastic scattering; alpha particles; Au target; optical model analysis.

PACS No. 24·10 Ht, 25·60 – t, 25·60 Cy

1. Introduction

A comprehensive data set covering a large E and A ranges followed by a systemic optical model analysis does not exist for the alpha-nucleus interaction. The data for the alpha-nucleus system are either limited in the angular range measured or in the E (and A) range covered (Singh and Schwandt 1976; Gregoire and Grotowski 1978). With lighter targets and at lower energies ($E < 40$ MeV) one often encounters the 'anomalous large angle scattering' phenomenon. This peculiar feature hampers determination of optical model parameters from the data (Eberhard *et al* 1976; Takigawa and Lee 1977). At higher energies ($E > 100$ MeV) where 'rainbow scattering' occurs, if the data includes the 'rainbow angle' then unique determination of the optical model parameters is possible (Goldberg and Smith 1972; Goldberg *et al* 1974; Wall *et al* 1978; Put and Paans 1977; Dalbra *et al* 1978). Some successful attempts have already been made to deduce global optical model parameters for $E \sim 90$–172 MeV (Dabrowski and Friendl 1981). Significant progress has also been made to calculate the alpha-nucleus optical potential from a microscopic approach (Friedman *et al* 1981; Kobos *et al* 1982; Gupta and Sinha 1984). It is desirable to have a data set covering a large E and A ranges, followed by a systematic and consistent optical model analysis, both macroscopic and microscopic not only to explain the elastic scattering data but also the inelastic scattering and transfer reactions.

We have, in the present study, measured the angular distribution for the elastic

scattering of 36 MeV alphas from gold. Section 2 gives the experimental procedure and results and §3, the optical model analysis of the data.

2. Experimental procedure and results

2.1 *Experimental setup*

An unanalyzed α-particle beam (36 MeV) from the variable energy cyclotron (VEC) at Calcutta was transported and focussed onto a $\sim$ 90 cm diameter scattering chamber (Chintalapudi *et al* 1978). The beam spot on the target was $\sim$ 6 mm in diameter. Three Si(Li) detectors (1–3 mm thickness) were placed, 10° apart, on the movable arm of the scattering chamber. Another Si(Li) detector (thickness $\sim$ 1 mm) was kept on the other arm which was kept fixed throughout the measurement. This served as the monitor detector. The solid angles subtended by the detectors were of the order of 10^{-4} sr and the angles of acceptance were $\pm 0{\cdot}3°$. For the whole measurement the ratio of the elastic peak yield as measured by the monitor detector kept at $\theta = 27{\cdot}5°$ to the current integrator counts remained a constant to within 1%, indicating negligible beam wandering (position and angle changes) on the target. The target was a self-supporting foil of gold (thickness $\sim$ 600 μg/cm^2). The signals from the detectors, processed by a system of charge sensitive preamplifier and spectroscopy amplifier, were fed to the ADC of the multichannel analyzer through a multiplexer unit. The overall energy resolution was $\sim$ 200 keV mainly attributed to the intrinsic beam energy spread from the machine. The beam current was measured by an ORTEC current integrator. An appropriate secondary electron suppressor measured the charge collected by the Faraday cup.

2.2 *Beam energy measurement*

This being one of the early experiments using the VEC, the energy of the cyclotron beam was determined by measuring the angular distribution of the α-particles scattered from ^{12}C target, going to the ground state (0 MeV) and the first excited state (4·43 MeV). By combining the pulse heights (channel numbers as measured by the MCA) corresponding to the elastic and inelastic peaks and employing the kinematic relations it is possible to deduce the beam energy (Heymann and Keizer 1963). The energy of the α-particle after scattering from ^{12}C target is given as

$$\begin{aligned} E_s(\theta) &= [M_P E_I^{1/2}\cos\theta + \{M_P^2 E_I \cos^2\theta \\ &\quad + (M_P + M_T)[(M_T - M_P)E_I - M_T E_x]\}^{1/2}]^2/(M_T + M_P)^2 \\ &= (\text{Channel number}) \times A + B \\ &\qquad\qquad (\text{MeV}) \quad (\text{MeV}) \end{aligned} \tag{1}$$

where E_I, E_S are the incident and scattered energy in MeV (in lab); M_T, M_P the target (^{12}C) and projectile (^{4}He); $E_x = 0$ and 4·43 MeV; θ is the scattering angle and A and B are calibration constants for the MCA. Figure 1 shows a least square fit to the channel number *vs* θ data with A, B and E_I as variable parameters. The best fit values are given as $E_I = 35{\cdot}81 \pm 0{\cdot}27$ MeV; $A = 0{\cdot}0718 \pm 0{\cdot}0004$ MeV and $B = -71{\cdot}287 \pm 0{\cdot}423$ MeV. When a small correction term θ_c was added to θ in the fitting process, it came out to be close to zero, indicating θ measured has negligible zero error.

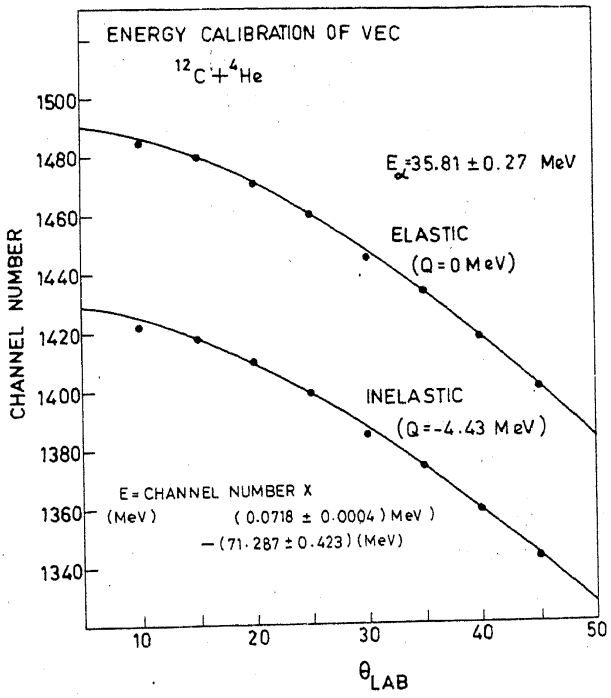

Figure 1. Energy calibration of VEC. Plot of channel numbers corresponding to elastic ($E_x = 0$ MeV) and inelastic peaks ($E_x = 4{\cdot}43$ MeV) for alpha scattering from ^{12}C *vs* θ.

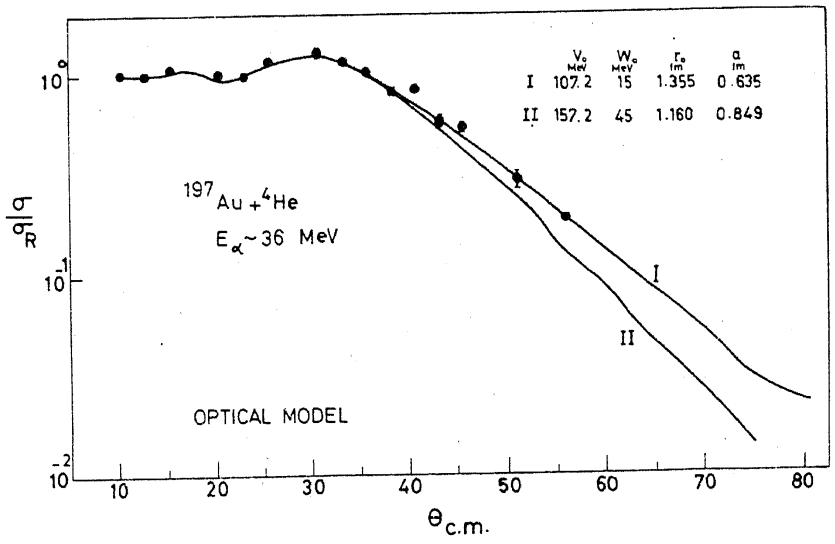

Figure 2. Angular distribution for elastic scattering of ~ 36 MeV alphas from gold plotted as ratios to Rutherford cross-section. The optical model fits to the data using I and II (as discussed in the text) are shown as continuous curves.

2.3 *Elastic scattering from ^{197}Au*

Elastic scattering from gold target was measured in the angular range $\theta \sim 10$–$56°$. The resulting angular distribution is given in figure 2 plotted as ratio to Rutherford cross-section. The data exhibit the familiar Fresnel diffraction pattern. Using the relation

$$Y(\theta) = \sigma_R(\theta) N_t N_\alpha d\Omega \qquad (2)$$

where $Y(\theta)$ the elastic yield at θ, N_t the largest atoms/cm^2, N_α the number of α particles, $d\Omega$ the solid angle subtended by the detector and $\sigma_R(\theta)$ the Rutherford cross section, the elastic yield at $\theta = 10$ and 12·5° have been normalized to $\sigma_R(\theta)$ to get the $N_t\,d\Omega$ product. Subsequently this value of $(N_t d\Omega)$ was used to determine $\sigma(\theta)$ at other angles.

The overall absolute error in $\sigma(\theta)$ values is estimated to be $\pm 10\%$ which includes uncertainties due to counting statistics, current measurement, and normalization to Rutherford cross-section.

3. Analysis

While analysing the data using the optical model we followed two prescriptions to extract the real potential parameters

(I) Gupta and Murthy (1982) have parametrized the real potential volume integrals J_R for projectiles with $A_P \leqslant 6$ for energy per nucleon up to 60 MeV. From this we deduced the J_R to be 297 MeV fm^3 for the gold plus alpha system at 36 MeV. From 42 MeV alpha scattering for targets with $A \leqslant 40$–68, Papanicolas *et al* (1982) have shown that the radius at which the real potential becomes 2·4 MeV, $R_{2\cdot4}$, is a well determined quantity. This radius is in fact very close to the strong absorption radius value. We have extended this concept to other α energies and A ranges. Starting from Perey and Perey (1976) compilation and using other recent α optical model analyses (Dabrowski and Friendl 1981; Friedman *et al* 1980; Wiktor *et al* 1981) we determined the $R_{2\cdot4}$ values for ^{27}Al, ^{58}Ni, ^{90}Zr and ^{208}Pb targets for $E \sim 20$–170 MeV. From figure 3, it is observed

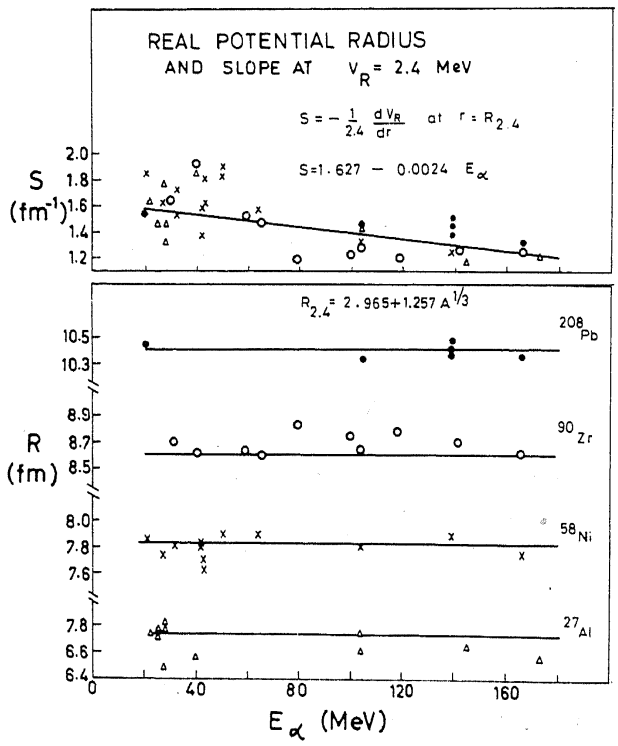

Figure 3. Systematics concerning $R_{2\cdot4}$ at $V_R = 2\cdot4$ MeV and S at $V_R = 2\cdot4$ MeV at various alpha energies for ^{27}Al, ^{58}Ni, ^{90}Zr, ^{208}Pb targets.

that the $R_{2\cdot4}$ values for a given target are almost energy independent. The energy averaged $R_{2\cdot4}$ values fit very well with the relation

$$2\cdot965 + 1\cdot2457\, A^{1/3}. \tag{3}$$

We also looked into the systematics of the slope

$$S = \left(\frac{1}{V_R(2\cdot4)} \frac{\mathrm{d}V_R}{\mathrm{d}r}\bigg|_{R=2\cdot4} \right) \tag{4}$$

for various A and E values. In figure 3 are plotted the S values for the targets mentioned above. It is seen that the S values are not strongly dependent on the A value of the target and their variation with E can be fitted with an expression

$$S = 1\cdot627 - 0\cdot0024\, E. \tag{5}$$

For a Woods-Saxon form for the real potential, we know

$$J_R = \frac{\pi}{3} V_0 r_0^3 \left[1 + \frac{\pi^2 a^2}{R^2} \right], \tag{6}$$

$$R_{2\cdot4} = a \ln \left(\frac{V_0 - 2\cdot4}{2\cdot4} \right) + R, \tag{7}$$

$$S = \frac{1}{a} \left[\frac{\exp\left(\frac{R_{2\cdot4} - R}{a} \right)}{1 + \exp\left(\frac{R_{2\cdot4} - R}{a} \right)} \right], \tag{8}$$

where $V_R(r) = V_0 \Big/ \left[1 + \exp\left(\frac{r - R}{a} \right) \right]$

and $R = r_0 A_T^{1/3}$ (A_T = target).

Using the J_R, $R_{2\cdot4}$ and S values for the $^{197}Au + {}^4He$ system at $E_\alpha \sim 36$ MeV, and by an iterative technique, we have deduced $V_0 = 107\cdot2$ MeV; $r_0 = 1\cdot355$ fm; $a = 0\cdot635$ fm.

(II) Srivastava *et al* (1983) have given empirical expressions for the mean square radius

$$\langle r^2 \rangle = \left[\frac{3}{5} R^2 \left(1 + \frac{7}{3} \frac{\pi^2 a^2}{R^2} \right) \right], \tag{9}$$

and the equivalent sharp radius (ESR)

$$= R \left(1 + \frac{\pi^2 a^2}{R^2} \right)^{1/3} \tag{10}$$

as a function of A at $E \sim 30$ MeV/nucleon. Assuming these to be energy independent and using the values $\langle r^2 \rangle = 37\cdot3$ fm^2 and ESR $= 7\cdot084$ fm for the $^{197}Au + {}^4He$ system deduced from their work, in conjunction with J_R (as given above) we have determined as before (using (6), (9) and (10)) $V_0 = 157\cdot2$ MeV, $r_0 = 1\cdot160$ fm and $a = 0\cdot849$ fm.

Having determined the real potential parameters as discussed above, we kept them fixed in fitting the $^{197}Au + {}^4He$ angular distribution data, using the optical model. The

radius and diffuseness parameters of the imaginary potential,

$$W_I(r) = W_0 / \left[1 + \exp\left(\frac{r-R}{a} \right) \right]$$

were kept at their respective real potential values. Only the depth, W_0, of the imaginary potential was varied (grid search) to fit the data. The W_0 values for the best fits are 15 and 45 MeV for I and II for the real part. The fits are shown in figure 2. The theoretical fit employing I for the real potential reproduces the experimental data better than the one using II. Using I, we get the reaction cross-section to be 1483 mb.

4. Conclusions

We have presented the details of the differential cross-section measurements for the elastic scattering of 36 MeV alphas from gold target. We have proposed two schemes to determine the real potential parameters. The optical model fit to the data has been carried out using both these prescriptions. Further work (involving more measurements) is necessary to arrive at a definite conclusion regarding the suitability of the two prescriptions and to decide about possible improvements to the two schemes.

References

Chintalapudi S N, Barde M L and Murthy G S N 1978 *Proc. Nucl. Phys. Solid State Phys (India)* **B21** 344
Dabrowski H and Friendl L 1981 *Acta Phys. Polon.* **B12** 703
Dalbra Th. *et al* 1978 *Phys. Rev.* **C18** 1237
Eberhard K A *et al* 1976 *Phys. Rev.* **C14** 548
Friedman E, Gils H J, Rebel H and Pesl R Karlsruhe 1980 KfK 3038
Goldberg D A and Smith S M 1972 *Phys. Rev. Lett.* **29** 500
Goldberg D A, Smith S M and Burdzik G F 1974 *Phys. Rev.* **C10** 1362
Gregoire G and Grotowski K 1978 *Proc. of the Second Louvain-Cracow seminar*
Gupta S K and Murthy K H N 1982 *Z. Phys.* **A307** 187
Gupta S K and Sinha B 1984 *Phys. Rev.* C (to be published)
Heymann G and Keizer R L 1963 *Nucl. Instrum. Meth.* **24** 125
Kobos A M, Brown B A, Hodgson P E, Satchler G R and Budzanowski A 1982 *Nucl Phys.* **A384** 65
Papanicolas C N, Sumner W U, Blair J S and Bernsteir A M 1982 *Phys. Rev.* **C25** 1296
Perey C M and Perey F G 1976 *At. Data Nucl Data Tables* **17** 1
Put L W and Paans A M J 1977 *Nucl. Phys.* **A291** 93
Singh P P and Schwandt P 1976 *Nukleonika* **21** 451
Srivastava D K, Basu D N and Ganguly N K 1983 *Phys. Lett.* **B124** 6
Takigawa N and Lee S W 1977 *Nucl. Phys.* **A292** 173
Wall N S, Cowley A A, Johnson R C and Kobos A M 1978 *Phys. Rev.* **C17** 1315
Wiktor S, Mayer Boricke C, Kiss A, Rogge M and Turek P 1981 *Acta Phys. Polon.* **B12** 491